

## Study of the impact of a new Drag Coefficient parameterization on the forecasting skill of an Ocean Model in the Aegean and Levantine Seas

Vassilis E. Kostopoulos\*, Eurydice Chrisagi, Sarantis Sofianos and Konstantinos G. Helmis

Department of Environmental Physics and Meteorology, Faculty of Physics, University of Athens, University Campus, Build. PHYS-5, Zografou, 15784, Athens, Greece.

**Abstract.** The aim of this work is to study the response of an ocean circulation model in the Eastern Mediterranean Sea, using a new drag coefficient formula based on observations at this area. Thirty twin simulation experiments of 5-days, using two different drag coefficient parameterizations were carried out by the Aegean-Levantine Eddy Resolving Model in a forecasting mode, covering all seasons and different wind field patterns for the year 2013. The new formula's forcing is based on measurements over the Aegean Sea while the second one is currently used by the model. The results show that the sea surface circulation was enhanced using the new parameterization giving wind stress values greater about 30%. The forecasting skill of the model was tested by comparing the daily sea surface temperature averaged estimations using the two formulas, with satellite observation records. Significant differences were found between the two formula's forecasts, both in space and in time, over the Aegean Sea and over the areas of the Levantine basin. Improved SST forecasts were found during spring over the Aegean Sea, while during autumn and winter, the differences were almost negligible. At summer, the bias was increased with undesired effects regarding SST forecasts, close to the coastal regions of the Eastern Mediterranean Sea that favor coastal upwelling.

**Keywords:** drag coefficient parameterization, Mediterranean Sea, sea surface circulation, ALERMO, forecasting skill.

### Introduction

It is well known that the ocean models are highly sensitive to the open boundary conditions of the air-sea interface. This issue remains a main subject in operational oceanography and numerous studies have assessed the impact of wind stress induced errors upon ocean forecasting models (e.g. Burillo et al. 2002) [1].

For numerical simulations, the surface fluxes are usually estimated using bulk formulas in a so called one-way air-sea interaction scheme (Rosati and Miyakoda 1988) [2]. This method has been extensively used in ocean forecasts and in coupled ocean-atmosphere studies. Other methods include the turbulence-based formulations (Fairall et al. 2003) [3] or prescribed flux fields (Korres 2003) [4] although the last one eliminates any feedback mechanism between the atmosphere and the ocean. By using bulk formulas, the momentum exchange at the sea surface is parameterized using the drag coefficient ( $C_D$ ) that is defined as,  $C_D = - \overline{u'w'}/\rho \cdot U^2$ , where  $\overline{u'w'}$  is the momentum flux at the sea

surface,  $\rho$  is the air density and  $U$  is the mean wind speed at a reference height, usually at 10 m ( $C_{D10}$ ). The drag coefficient has been found to increase approximately linearly with the wind speed at moderate and strong winds (e.g. Smith 1980) [5], depending on stability (e.g. Paulson 1970) [6]. The various regression equations from independent experiments, under neutral conditions, present considerable differences, usually related to the sea state (Drennan et al. 2003) [7]. Over the Aegean Sea which is characterized by relatively short spatial scales (up to  $10^2$  km), increased drag coefficient values were found, a factor of two compared to typical values measured over the ocean, possibly related to the variable fetch conditions (Kostopoulos and Helmis 2014) [8].

Regarding the ocean's response, it is reported from relative studies (e.g. Burillo et al. 2002) [1] that inconsistent surface forcing may result at misleading thermal content of the upper ocean as well as at horizontal patterns of the sea surface temperature (SST) due to horizontal advection processes, for short time scales forecasts (order of few days). Over the Aegean Sea which is a semi-enclosed basin with

\*Corresponding author: Vassilis E. Kostopoulos  
E-mail address: [vkostopoulos@phys.uoa.gr](mailto:vkostopoulos@phys.uoa.gr)  
DOI: <http://dx.doi.org/>

complex coastline (Fig. 1), the surface circulation has been proved to be significantly affected by the boundary mixing processes and especially from the momentum transfer across the air-sea interface (Sofianos et al. 2010) [9]. The aim of this study is to evaluate the forecasting differences of the ocean circulation forecasting system Aegean-Levantine Eddy Resolving Model (ALERMO) over the Aegean and the Levantine Seas, using two different

parameterizations for the drag coefficient; the one that is currently used by the model which is based on the Hellerman and Rosenstein's (1983) [10] formula and a new one resulting from field measurements over the Aegean Sea. The evaluation is based on comparison between satellite observation records of SST and the corresponding SST estimations from ALERMO using both formulas.

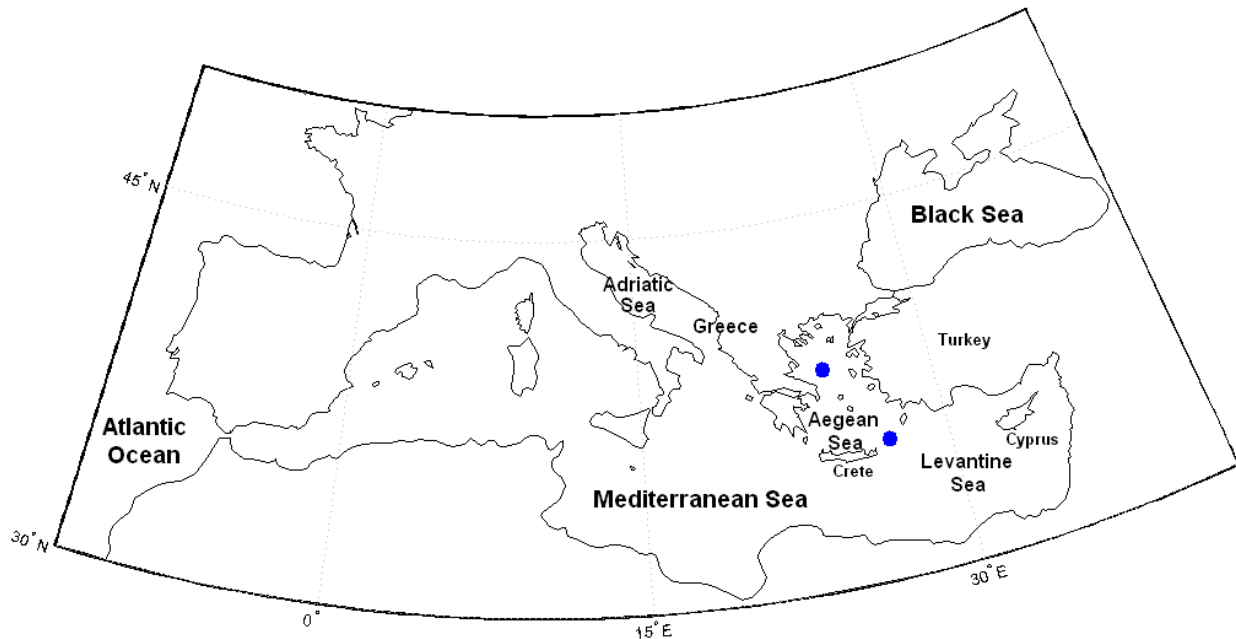


**Figure 1.** The areas of the Aegean and the Levantine Seas. The experimental sites where turbulent measurements took place are indicated with blue dots.

## Experimental Section

### The Eastern Mediterranean Sea

The Eastern Mediterranean Sea can be divided into two well distinguished greater areas: the Aegean and the Levantine Sea (Fig. 1). The Levantine Sea is the open, south-eastern area of the basin. The Aegean Sea is the northern part of the eastern Mediterranean Sea, an Archipelago characterized by its complex topography with approximately 3.000 islands and isles scattered between the main lands of Greece and Turkey. According to Sofianos et al. (2010) [9], the sea surface circulation patterns in the Aegean, present a seasonal character and they are associated with the seasonal wind field patterns as well as with the seasonal thermohaline characteristics. Regarding the SST, satellite observations from 1985 to 2006 indicate an intense spatial variability over the Aegean Sea during summer, with the highest SST changes found during August (Skloris et al. 2011) [11]. This variability is mostly attributed to the entering of fresh Black Sea Waters (BSW) from the northeast of the basin with maximum inflow during summer (Tzali et al. 2010) [12] and the seasonal north etesian winds (e.g. Rizou et al. 2013) [13] during the same period, that cause upward transport of deep cold water on the east coasts due to coastal upwelling and relevant

turbulent mixing processes (Sofianos et al. 2002) [14].

### The new bulk air-sea momentum flux parameterization

The proposed parameterization of the neutral drag coefficient ( $C_{DN10}$ ) is a function of the wind speed at 10 m height ( $U_{10}$ ) and it is based on recent turbulent flux measurements within the surface Atmospheric Boundary Layer (ABL) of the Aegean Sea, using eddy correlation analysis. Regarding the flux measurements, meteorological masts were installed close to the shoreline of two islands at northern (Skyros) and south-eastern (Karpathos) Aegean Sea of Greece (Fig. 1), during summer 2011 and 2012, equipped with sonic anemometers. In total, 226 hours of quality controlled observations were available for analysis, 55h from the north and 171h from the south-eastern Aegean. A detailed description of the two experimental sites, the instrumentation and data analysis can be found in Kostopoulos and Helmis (2014) [8]. According to the results of this work, the estimated  $C_{D10}$  values appeared to be characterized by higher values relative to the typical values measured over the ocean, regardless stability which was found to be near neutral on both sites ( $-0.04 < z/L < 0.2$ ). Based on the available data from the southern-eastern Aegean expedition, with 92 hours of observations (neutral

conditions only  $C_{DN10}$ ,  $C_{DN10}$  is given as an increasing linear function of the wind speed ( $U_{10}$ ), at 0.01 confidence level ( $t=0.12$ ,  $s_{xy}^2=0.34 \cdot 10^{-7}$ ), according to the following eq.1 (K&H formula).

$$C_{DN10} = c_0 + c_1 \cdot U_{10} \quad (1)$$

Where  $c_0$  and  $c_1$  coefficients are given at table 1 (first line). As neutral conditions were considered data with stability parameter ( $z/L$ ) absolute values less than 0.02, according to Karlsson's (1986) [15] classification. In Figure 2, this proposed parameterization of  $C_{DN10}$  is plotted as a function of the wind, along with the one based on Hellerman and Rosenstein (H&R) results. H&R formula which is currently used by the ALERMO model and has been widely used in ocean models is a second degree polynomial function of wind speed (eq.2), under neutral stability conditions.

$$C_{DN10} = c_0 + c_1 \cdot U_{10} + c_2 \cdot U_{10}^2 \quad (2)$$

Where  $c_0$ ,  $c_1$  and  $c_2$  coefficients are given at table 1 (second line). It is noted, that the H&R formula also includes the influence of air-sea temperature difference (eq.3, see also table 1 third line), so the comparison between the application of the linear regression formula (K&H) for  $C_{DN10}$ , with the more

complex H&R formula, is conducted assuming that air and sea close to the surface have the same temperature ( $\Delta T=0$ ).

$$C_{D10} = c_0 + c_1 \cdot U_{10} + c_2 \cdot U_{10}^2 + c_3 \cdot \Delta T + c_4 \cdot \Delta T^2 + c_5 \cdot \Delta T \cdot U_{10} \quad (3)$$

Where  $c_3$ ,  $c_4$  and  $c_5$  coefficients are given at table 1 (third line). The neutral stability assumption separates the influence of the wind speed from the influence of the temperature and it was noticed very clearly during both experiments over the Aegean Sea (Kostopoulos and Helmis 2014) [8].

The two formulas, according to table 1, give almost the same first order equation coefficient ( $c_1$ , linear slope). The slight change in the slope due to the second degree coefficient ( $c_2$ ) causes the estimated  $C_{DN10}$  values to be reduced less than 10% for wind speed values of the order of 20 m/s. This is the reason why in Figure 2, H&R line presents an almost linear pattern for winds up to 11m/s. The K&H formula gives a greater zero order coefficient ( $c_0$ , Y-intercept) by 30%. This means that for the average annual wind speed range over Aegean, the atmospheric forcing using the new formula will be greater by one third, under neutral conditions.

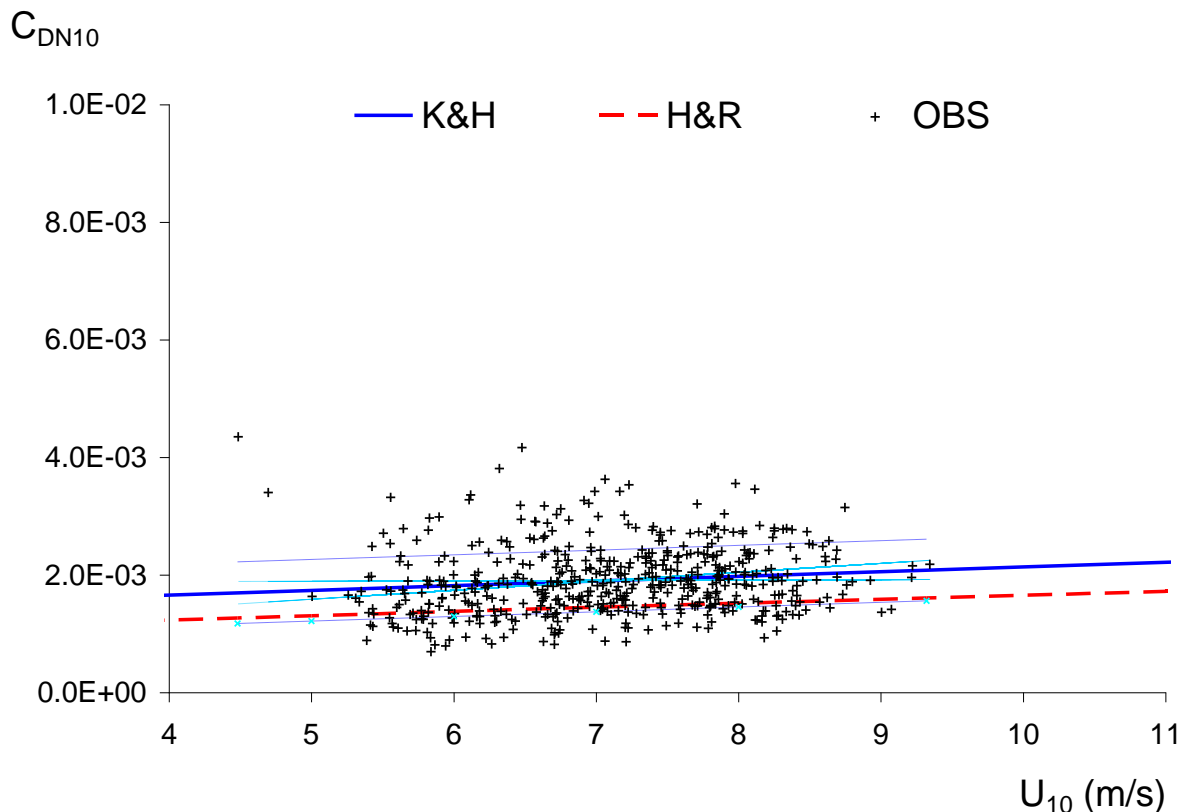


**Figure 2.** Scatter diagram between the measured neutral drag coefficient ( $C_{DN10}$ ) values and the wind speed from observations (+), the estimated by the diagram regression line (blue - solid line, K&H formula) and the Hellerman and Rosenstein (red - dotted line, H&R) formula as functions of wind speed ( $U_{10}$ ). The dotted blue and light blue lines correspond to the 0.01 confidence intervals for the slope ( $c_1$ ) and the axis intercept ( $c_0$ ) respectively of the regression.

**Table 1.** The drag coefficient ( $C_{DN10}$ ) formula's with the wind speed and air-sea temperature difference ( $\Delta T$ ) coefficients for K&H and H&R schemes.

$C_{DN10}$	$c_0$	$c_1 \cdot U_{10}$	$c_2 \cdot U_{10}^2$	$c_3 \cdot \Delta T$	$c_4 \cdot \Delta T^2$	$c_5 \cdot U_{10} \cdot \Delta T$
<b>K &amp; H</b>	$1.34 \cdot 10^{-3}$	$7.98 \cdot 10^{-5}$	-	-	-	-
<b>H &amp; R</b> $\Delta T=0$	$0.93 \cdot 10^{-3}$	$7.88 \cdot 10^{-5}$	$- 6.16 \cdot 10^{-7}$	-	-	-
<b>H &amp; R</b>	<b><math>0.93 \cdot 10^{-3}</math></b>	<b><math>7.88 \cdot 10^{-5}</math></b>	<b><math>- 6.16 \cdot 10^{-7}</math></b>	<b><math>8.68 \cdot 10^{-5}</math></b>	<b><math>- 1.20 \cdot 10^{-6}</math></b>	<b><math>- 2.14 \cdot 10^{-6}</math></b>

### Model and Data

The ALERMO (Aegean-Levantine Eddy Resolving Model) forecasting system (Korres et al. 2002) [16] covers part of the Eastern Mediterranean Sea (30.7°- 41.2° N, 20°- 36.4° E). It was first developed within the framework of the Mediterranean Forecasting System (MFS) (Tonani et al 2014 [17], Dombrowsky et al. 2009 [18]). It is based on the Princeton Ocean Model which is a sigma layer model. The model's horizontal resolution is approximately 3.5 km (1/30 degrees) and uses 25 logarithmic vertical distributed layers so the surface layer extends from few centimeters up to several meters depending on the region's variable bathymetry. The model is forced by the (1/10°) SKIRON atmospheric forecasting fields (Kallos 1997) [19] and is nested in the MyOcean forecasting system. More explicitly, the model's open boundary conditions use one way nesting with an (1/16°) Ocean General Circulation Model (OGCM) based on NEMO-OPA (Nucleus for European Modelling of the Ocean-Ocean Parallelise) version 3.4 (Madec et al. 2008) [20] that runs operationally and initialises ALERMO on a daily basis.

In order to investigate the effect of the use of the new parameterization for  $C_D$ , two twin simulation experiments (H&R $_{\Delta T=0}$  and K&H runs) were performed, implementing the corresponding drag coefficient formulas as functions of wind speed. Also two more, twin simulation experiments (H&R and K&H $_{\Delta T}$  runs) were performed, implementing the two formulas as functions of the air-sea temperature difference in addition to the wind speed. This was performed in order to investigate the influence of the stability at the model's forecast using the H&R formula, while the *ad hoc* implementation of the stability factors ( $c_4$ ,  $c_5$ ,  $c_6$ ) at K&H $_{\Delta T}$  formula proved to act favorable in the forecast's accuracy, as it is discussed in section 5.3.

The impact on the forecast was estimated by comparing the model's daily averaged estimated SST values for the first sigma ( $1\sigma$ ) layer that was used for validation, with satellite SST observations with a resolution of 6.5 Km (1/16 degrees). These daily mean records are the Copernicus SST operational product for the Mediterranean Sea (Nardelli et al. 2013) [21] and were interpolated to the model's grid in order to be compared with the model's results. Satellite SST products cover large areas and periods of time and were selected for the purposes of this work rather than other possibly available in situ

measurements like ARGO profiles or buoys data, since the latter provide scarce and local, comparing to the grid of the model, records that could mislead validation results.

The differences as well as the root mean square error (RMSE) were computed, for each grid and day of the test period. In addition, in order to investigate the response of the model's surface circulation, daily averages of the mean kinetic energy and surface horizontal velocity, temperature and salinity of the sea were estimated, along with the applied tangential stress, the drag coefficient and the wind at 10 m height, for all four case studies.

In total, one hundred fifty (150) days of forecast were examined from thirty 5-days simulation experiments that were carried out in a forecasting mode, for the years 2012- 2013. The selection of the test period was based on the goal of testing the forecasting skill of the model in annual basis in order to take into account all seasons and different wind field patterns. It is worth mentioning that minimum two runs per month for year 2013 were chosen, corresponded to moderate or strong wind periods according to the prevailing wind directions, as well as two more runs for year 2012, one during summer and one during the winter.

## Results and Discussion

### Surface circulation's response

The new parameterization formula induces enhanced surface forcing and this fact was reflected at the estimated kinetic energy (KE) values of the surface circulation structures of Levantine and Aegean Seas. The mean increase of the drag coefficient values for all runs was 33% and this increase corresponds to 21% increase of the mean calculated surface KE value. According to table 2, the relative KE difference between the two methods, present a rather small seasonal variation besides a winter minimum which could be related to the role of the thickness of the sea mixed layer over the Aegean (Kara et al. 2009) [22] that can influence a variety of upper ocean processes, including air-sea exchange (e.g. Chen et al. 1994) [23]. In fact, Kara et al. 2009 [22] revealed that the mixed layer depth of the Aegean Sea is deeper during winter than the rest of the year so enhanced wind forcing could imply increased surface kinetic energy but vertically distributed within a deeper layer hence the winter relative first 10m KE difference minimum.

The circulation patterns remained unchanged even though the mean increase of the surface KE values for all runs locally reached twice higher percentages than the overall average (Fig. 3), leading to the enhancement of the existing surface structures.

Small changes in size, shape and position of some large structures were observed and it is believed that it is also due to shifts, that locally increases up to 60% of the KE values are seen in Figure 3.

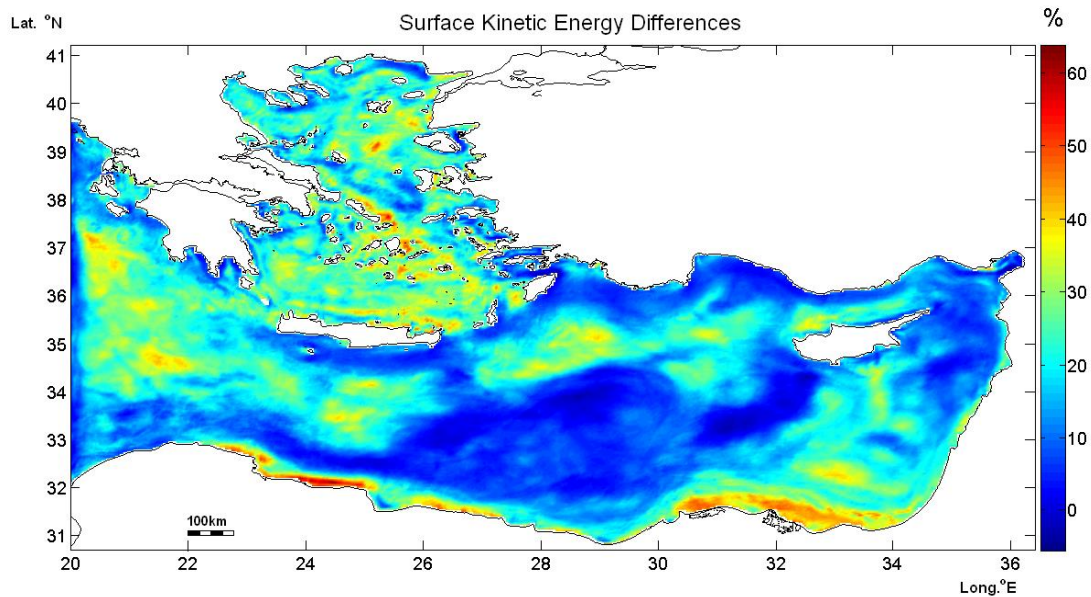


**Figure 3.** Sea Surface (first 10m) Kinetic Energy (KE) percentage relative differences between the two formulas runs  $[(K\&H-H\&R_{\Delta T=0})/H\&R_{\Delta T=0}]$ , for the test period.

**Table 2.** The seasonal percentage differences of the spatial averaged kinetic energy (KE) of the first 10 m of the sea, between K&H and H&R $_{\Delta T=0}$  schemes  $[(K\&H-H\&R_{\Delta T=0})/H\&R_{\Delta T=0}]$  for all runs.

KE Difference	Winter	Spring	Summer	Autumn
%	16	23	21	24

### Effects on model's predictions

The induced enhancement in surface circulation, lead to local and seasonal differences in the forecasting skill of the ALERMO. In Figure 4, the estimated RMSE of SST differences for H&R $_{\Delta T=0}$  and K&H runs is presented as time series while Figure 5 gives the average SST percentage RMSE differences between the two schemes forecasts of all forecast days and averaged over areas of 0.5x0.5 degrees. It is evident from both figures that the two forecasts present differences both in space and time. As seen in Figure 5, K&H runs present improved SST forecasts at the west, north and southern coasts of the Aegean Sea and enhanced bias at the eastern coasts. The RMSE for all cases gave seasonal variation with increasing values which were found mostly during summer but also earlier on spring (Fig. 4). This is also evident in the corresponding seasonal spatial differences of RMSE values seen in figures 7b and 8b that can be clearly identified as dominant annual contributions according to Figure 5.

During spring, the K&H forecast presents lower RMSE values than the corresponding H&R's ones and the opposite during summer (Fig. 4). The seasonality of the RMSE differences are also reflected in terms of seasonal averages which are presented in table 3 as well as from the corresponding values of the two additional runs for the year 2012, as seen in Figure 4. The total RMSE on the other hand, present negligible differences for all case studies (Table 3), hiding the different seasonal effects of the new parameterization scheme to the model's predictions. It should be also noticed that according to table 3, when stability is included in the  $C_{DN10}$  parameterization scheme, the RMSE gives much smaller changes, seasonally and on average, for both schemes.

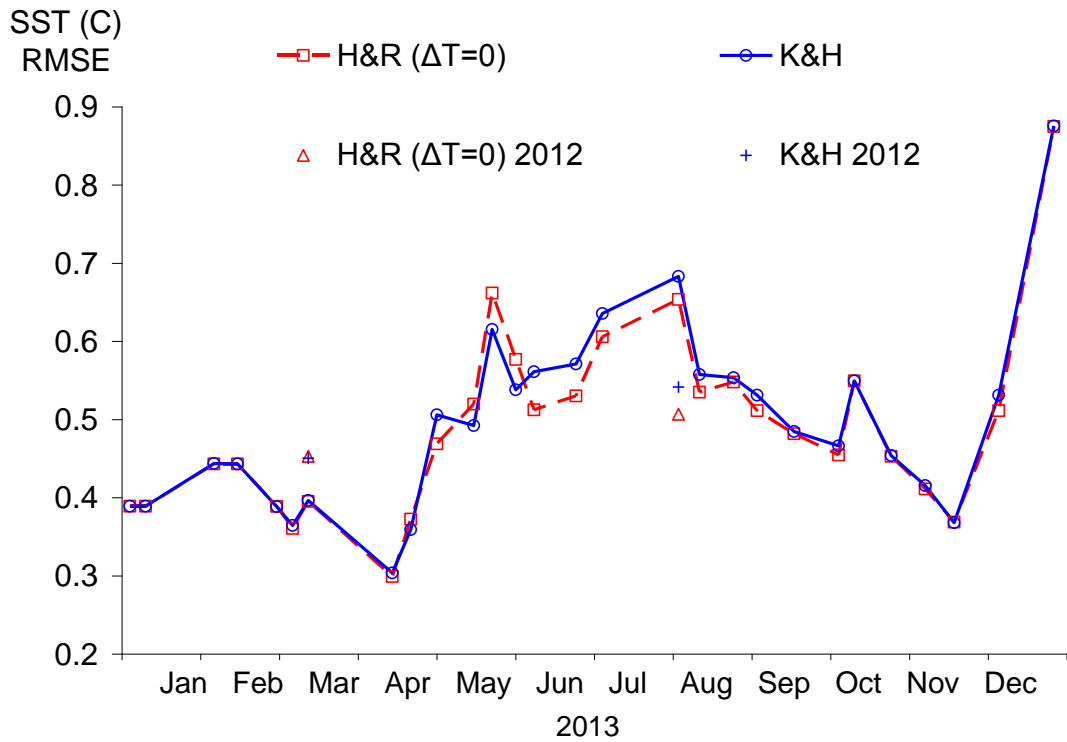


**Figure 4.** RMSE time series of differences with the satellite SST observations for the test period, based on K&H formula (blue - solid line) and H&R<sub>ΔT=0</sub> (red - dotted line) forecasts.

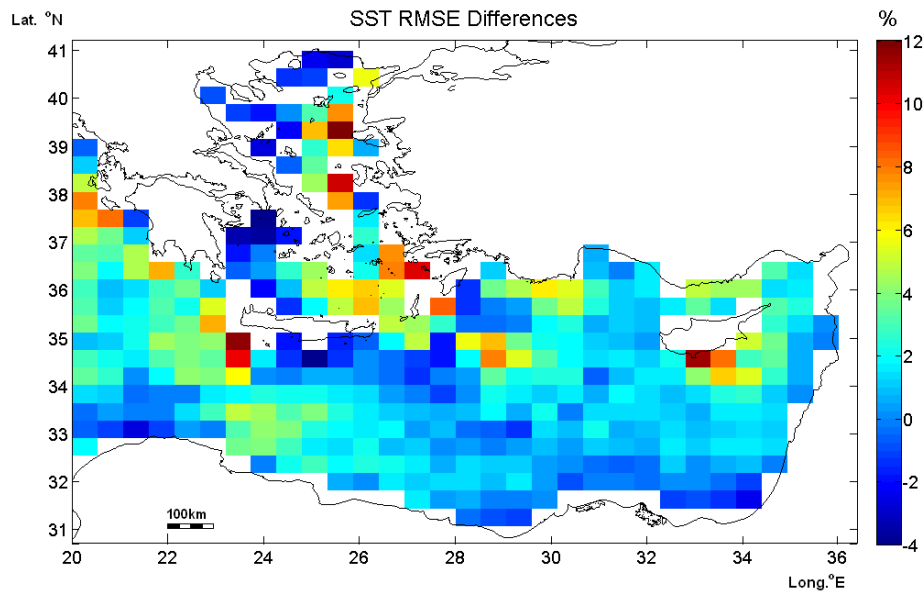


**Figure 5.** Percentage relative differences between K&H and H&R<sub>ΔT=0</sub> forecasts [RMSE with the satellite SST observations,  $(K\&H - H\&R_{\Delta T=0}) / H\&R_{\Delta T=0}$ ] for all runs, averaged over areas of 0.5x0.5 degrees. Relative improvement is presented with blue and induced bias with red colors.

**Table 3.** Total (all runs) and seasonal, spatial averaged RMSE of the differences with the satellite SST observations, for all cases studies.

SST RMSE	Total	Winter	Spring	Summer	Autumn
<b>H&amp;R<sub>ΔT=0</sub></b>	0.4866	0.4069	0.4874	0.5478	<b>0.5069</b>
<b>K&amp;H</b>	0.4924	0.4073	0.4822	0.5713	<b>0.5096</b>
<b>H&amp;R</b>	0.4843	0.4066	0.4830	0.5429	<b>0.5074</b>
<b>K&amp;H<sub>ΔT</sub></b>	<b>0.4897</b>	<b>0.4072</b>	<b>0.4774</b>	<b>0.5651</b>	<b>0.5099</b>

During spring and summer, the two forecasts presented significant spatial differences. According to Figure 6 during late spring (June 15 2013) and Figure 8a during summer, under the influence of the etesian winds, in coastal regions that are favorable for coastal upwelling (east Aegean close to Turkey, western Aegean close to Greece and south of Cyprus coasts) the RMSE values are increased locally on both schemes forecasts. The use of K&H formula in fact increased the relative bias with even cooler surface waters observed over these areas up to 1°C locally (Fig. 6). This reveals a straight forward impact of the use of increased forcing by enhanced coastal surface horizontal advection processes which are relative to the observed upwelling mechanism. It

is also obvious in Figure 6 that due to horizontal advection, these surface waters are circulated from the corresponding surface patterns away from source areas. This was also evident at the surface temperature front at Dardanelles Strait where the source of BSW is located (Fig. 6) and boundaries where significantly altered constantly during the whole year (not shown). These facts allows us to understand the nature of the forecast's differences, mainly due to the combination of horizontal advection through various circulation patterns and mixing of surface waters, far from intense SST variability sources and thus not due to air-sea heat fluxes.

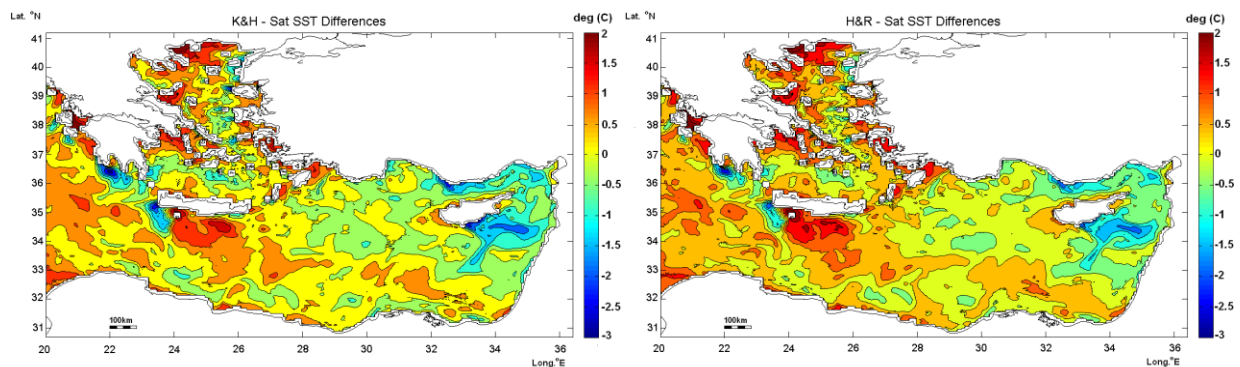


**Figure 6.** Contour plot (0.5°C level step) of spatial SST forecast differences comparing to the satellite observations (model-satellite), using K&H (left) and H&R<sub>ΔT=0</sub> (right) formula, for June 15 2013.

This could explain the appearance of cooler surface waters using K&H formula (Fig. 6 and 7b) during spring, when the etesian winds start to build up, due presumably to a better recirculation of the corresponding water masses over the Aegean, since lower bias exists comparing to H&R<sub>ΔT=0</sub> formula. There is improvement of increased deviations (warmer waters) from the satellite records using H&R scheme, according to figures 7a and 7b, in the

complex eastern Greek coastline areas as well as in most northern coasts of the Aegean. Similarly, reduced bias was found also in the Levantine Sea, south from Crete Island and on the north-easterly Africa coasts during spring. So, it becomes evident that the seasonal spatial differences on the SST forecast are strongly related to horizontal advection of cooler surface waters that originate from the Aegean towards the particular areas.

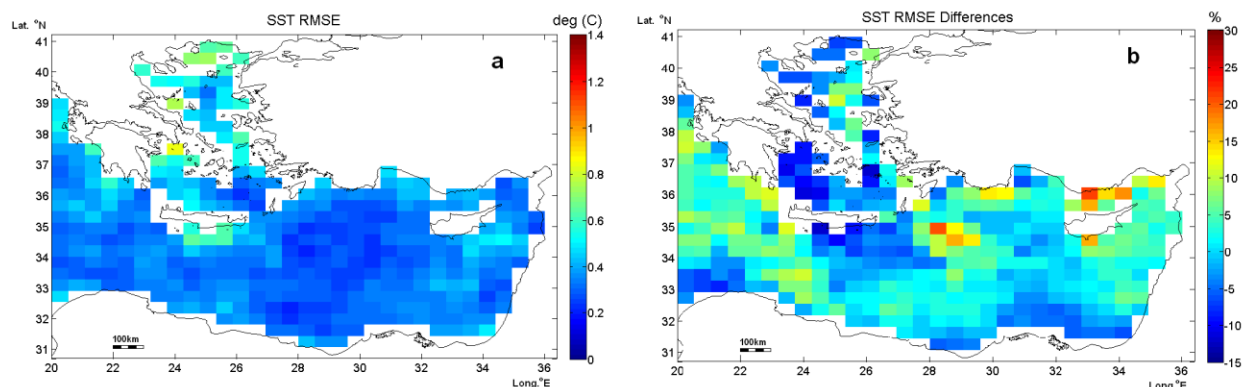


**Figure 7.** Spring averaged model output differences (RMSE) with the satellite SST observations for H&R<sub>ΔT=0</sub> forecast on the left (a), averaged over areas of 0.5x0.5 degrees. Similar averaged, percentage relative differences between K&H and H&R<sub>ΔT=0</sub> SST forecasts [ $RMSE, (K\&H-H\&R_{\Delta T=0})/H\&R_{\Delta T=0}$ ] are shown on the right (b).

Relative improvement is presented with blue and induced bias with red colors.

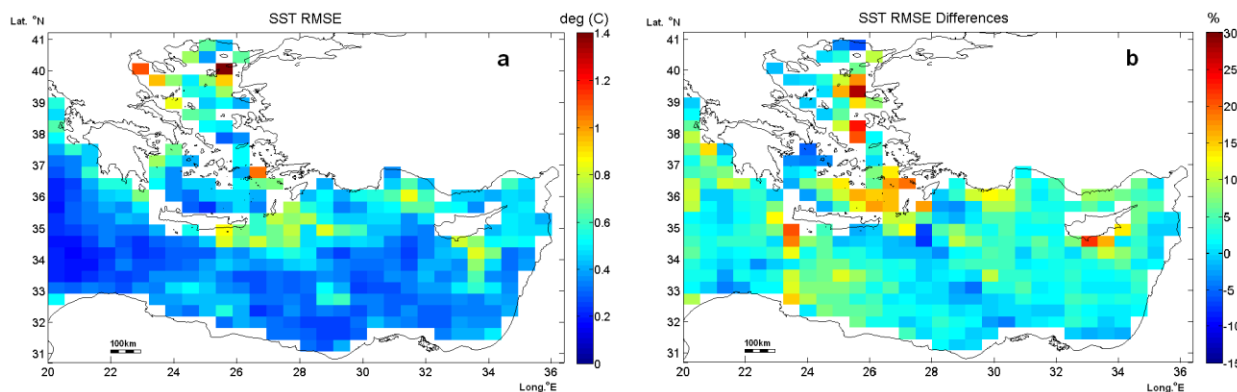


**Figure 8.** Summer averaged model output differences (RMSE) with the satellite SST observations for  $H\&R_{\Delta T=0}$  forecast on the left (a), averaged over areas of  $0.5 \times 0.5$  degrees. Similar averaged, percentage relative differences between K&H and  $H\&R_{\Delta T=0}$  SST forecasts [ $RMSE, (K\&H - H\&R_{\Delta T=0}) / H\&R_{\Delta T=0}$ ] are shown on the right (b). Relative improvement is presented with blue and induced bias with red colors.

The improved forecasts during spring as seen in figure 7b, locally goes up to more than 10%, regarding the seasonal averaged RMSE values averaged over areas of  $0.5 \times 0.5$  degrees. During the single 5-days forecasts and without spatial averaging, the relative improvements reached values up to 25% over the above mentioned areas. On the other hand, the induced errors in the vicinity of the coastal upwelling areas during summer (Fig. 8b), grew up to 30% (seasonal average over  $0.5 \times 0.5$  degrees) and up to 50% in 5-days forecasts in few areas. It should although be mentioned that only at the northeastern coasts, enhanced differences corresponded to locations of increased error using  $H\&R_{\Delta T=0}$  formula, according to Figures 8a and 8b.

During winter and autumn, the RMSE values for all cases were reduced about 30% in average (Fig. 4). The differences between the two forecasts were almost negligible during winter and very limited during autumn reflecting the absence of upwelling processes as source of cooler surface waters due to the persistence of the etesian winds, that combined with BSW inflow minimum reduce the basic causes of extended spatial SST variation over the Aegean and thus the consequent bias. In fact, major changes were found between the two forecasts during winter around the BSW front in the Aegean while during autumn, the variations were related mostly to the effects relative to the decaying etesian winds and the corresponding circulation patterns.

### Stability influence

The role of stability was proved to act favorable on the forecast skill of the model mainly over the Aegean and its eastern coasts and not favorable over the open Levantine Sea according to Figure 9. Due to

the seasonal east-west orientation of the SST variance over the Aegean during summer, etesian winds from north-western directions can be advected under relatively large angles towards the corresponding SST gradients of few degrees over 100 km. The drag coefficient values downwind the gradient were expected to be depressed (table 3, line 3) since the air flows from warmer to cooler surface waters, due to the increasing stability (Small et al. 2008) [24]. The effect of variable fetch conditions and intense SST variability in the observed air-sea temperature differences and the resulting stability conditions over the region was pointed out from Kostopoulos and Helmis (2014) [8], using buoys records and turbulent measurements within the marine ABL over the Aegean. Regarding the model's wind forcing sensitivity to stability, under typical SST gradients regarding location (e.g. Figure 6) and strength, the effect summed up to reduce the applied surface stress up to 50% during summer downwind SST gradient in the eastern coasts of the Aegean Sea as well as southerly of the western Cretan Straits (Fig. 9). This consequently seems to lead to relative depression of the local influenced mechanisms of coastal pumping and it is believed to be the reason for the improvements that are presented in Figure 9 over the eastern coasts of the Aegean. The related improvements locally reached up to about 15% using  $H\&R$  or  $K\&H_{\Delta T}$  scheme, during summer and it is noticed that the described improvement presented its maximum in the vicinity of the BSW inflow temperature front and the east coasts, areas where maximum RMSE values were found using both schemes under neutral conditions (Fig. 8a).

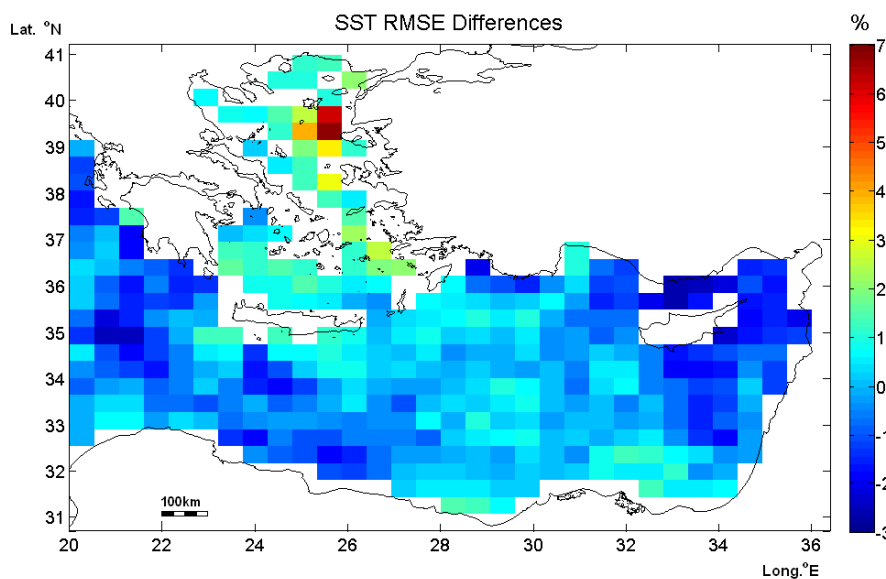


**Figure 9.** Percentage relative differences between K&H and K&H <sub>$\Delta T$</sub>  forecasts [RMSE with the satellite SST observations,  $(K\&H - K\&H_{\Delta T})/K\&H$ ] for all runs, averaged over areas of 0.5x0.5 degrees. Relative improvement is presented with red and induced bias with blue colors.

## Conclusions

An observation-based drag coefficient formula for momentum transfer at the air-sea interface, from turbulence measurements within the surface marine ABL of the Aegean Archipelago was implemented. A comparison between the results of the ocean circulation forecasting system ALERMO, using the (H&R) formula and a new (K&H) parameterization scheme and satellite SST observation records, was conducted. The new parameterization results to stronger surface forcing compared to H&R scheme. A general enhancement of the kinetic energy of surface circulation of the order of 20% was observed while the circulation patterns did not present changes. Regarding the RMSE values between the model estimations and the SST observations, it was found that they increase during spring and summer due to the complexity of the circulation and the associated SST during this period of the year. Numerous differences were found in the forecasting skill using both schemes during these periods, presumably as the result of horizontal advection and mixing of different temperature surface waters, far from intense SST variability sources, like coastal upwelling areas. During spring, the forecast skill was improved in the whole domain and in some areas the improvement reach locally up to 25%, in single 5-days runs. On contrary, during summer the new scheme induced increased seasonal errors up to 30% in the vicinity of coastal upwelling areas mostly at the eastern coasts of the Aegean. Over these regions and near the north Aegean temperature front, the stability was found to improve locally the model's accuracy. The results also show the need for further investigation of coastal processes and the oceanic response to intense wind forcing in shallow areas.

## Acknowledgements

This research has been co-financed by the European Union (European Social Fund - ESF) and Greek national funds through the Operational Program "Education and Lifelong Learning" of the National Strategic Reference Framework (NSRF) - Research Funding Program: Heracleitus II, Investing in knowledge society through the European Social Fund.

## References

1. Burillo IA, Caniaux G, Gavart M, De Mey P, Baraille R. Assessing ocean-model sensitivity to wind forcing uncertainties. *Geophys Res Lett.* 2002 Sep; 29(18):51-4.
2. Rosati A, Miyakoda K. A general circulation model for upper ocean simulation. *J Phys Oceanogr.* 1988 May; 18:1601-26.
3. Fairall CW, Bradley EF, Hare JE, Grachev AA, Edson JB. Bulk Parameterization of Air-Sea Fluxes. Updates and verification for the COARE Algorithm. *J Climate.* 2003 May; 16:571-91.
4. Korres G, Lascaratos A. A one-way nested eddy resolving model of the Aegean and Levantine basins: implementation and climatological runs. *Ann Geophys.* 2002 Jan; 21(1):205-20.
5. Smith SD. Wind Stress and Heat Flux over the Ocean in Gale Force Winds. *J Phys Oceanogr.* 1980 May; 10:709-26.
6. Paulson CA. The Mathematical Representation of Wind Speed and Temperature Profiles in the Unstable Atmospheric Surface Layer. *J Appl Meteor.* 1970 Dec; 9:857-61.

7. Drennan WM, Graber HC, Hauser D, Quentin C. On the wave age dependence of wind stress over pure wind seas. *J Geophys Res.* 2003 Mar; 108(C3):8062.
8. Kostopoulos VE, Helmis CG. Flux measurements in the surface marine Atmospheric Boundary Layer over the Aegean Sea. *Sci Total Environ.* 2014 Jul; 494-495: 166-76.
9. Sofianos S, Skliris N, Vervatis V, Olson D, Kourafalou V, Lascaratos A, et al. On the Forcing Mechanisms of the Aegean Sea Surface Circulation. *European Geosciences Union General Assembly*; 2015 Apr 12-17; Vienna (AT). 2015. Geophys Res Abstr 17
10. Hellerman S, Rosenstein M. Normal monthly wind stress over the World Ocean with error estimates. *J Phys Oceanogr.* 1983 Mar; 13:1093-104.
11. Skliris N, Sofianos S, Gkanasos A, Axaopoulos P, Mantziafou A, Vervatis V. Long-term sea surface temperature variability in the Aegean Sea. *Adv Limnol Oceanogr* 2011 Nov; 2(2):125-39.
12. Tzali M, Sofianos S, Mantziafou A, Skliris N. Modelling the impact of Black Sea water inflow on the North Aegean Sea hydrodynamics. *Ocean Dynam.* 2010 Jun; 60(3):585-96.
13. Rizou D, Flocas H, Bartzokas A, Helmis CG in: Lekkas TD, editor. On the link between Indian summer monsoon and the Etesian pattern over the Aegean Sea. CEST 2013: *Proceedings of the 13th International Conference on Environmental Science and Technology*; 2013 Sep 5-7; Athens (GR). *University of the Aegean.* 2013. Available from: [https://www.researchgate.net/publication/256505917\\_On\\_the\\_link\\_between\\_Indian\\_summer\\_monsoon\\_and\\_the\\_Etesian\\_pattern\\_over\\_the\\_Aegean\\_Sea](https://www.researchgate.net/publication/256505917_On_the_link_between_Indian_summer_monsoon_and_the_Etesian_pattern_over_the_Aegean_Sea)
14. Sofianos S, Johns W, Lascaratos A, Murray S, Olson D, Theocharis A. Draft Report of the Aegean Sea Workshop. *Proceedings of the Aegean Sea Workshop*; 2002 Oct 8-10; Rhodes (GR). 2002. Available from: [http://www.oc.phys.uoa.gr/workshop/Aegean\\_Draft\\_Report\\_f.htm](http://www.oc.phys.uoa.gr/workshop/Aegean_Draft_Report_f.htm)
15. Karlsson S. The Applicability of Wind Profile Formulas to an Urban-Rural Interface Site. *Bound-Lay Meteorol.* 1986 Mar; 34:333-55.
16. Korres G, Lascaratos A, Sofianos S, Kallos G. The ALERMO ocean circulation forecast system, *3rd EuroGOOS Conference*; 2002 Dec; Athens (GR).
17. Tonani M, Teruzzi A, Korres G, Pinaridi N, Crise A, Adani M et al. 2014. The Mediterranean Monitoring and Forecasting Centre, a component of the MyOcean system. *Proceedings of the Sixth International Conference on EuroGOOS*; 2011 Oct 4-6. Sopot (PL). Eurogoos Publication. 2011.
18. Dombrowsky E, Bertino L, Brassington GB, Chassignet EP, Davidson F, Hurlburt et al. GODAE Systems in operation. *Oceanography.* 2009;22(3):83-95.
19. Kallos G. The Regional weather forecasting system SKIRON. *Proceedings, Symposium on Regional Weather Prediction on Parallel Computer Environments*; 1997 Oct 15-17; Athens (GR). 1997.
20. Madec G. NEMO reference manual, ocean dynamics component: NEMO-OPA. *Preliminary version. Institut Pierre-Simon Laplace (FR).* 2008. 399p. Report No.: 27. ISSN No.: 1288-1619. Available from: <http://www.nemo-ocean.eu/About-NEMO/Reference-manuals>
21. Nardelli B, Tronconi C, Pisano A, Santoleri R. High and Ultra-High resolution processing of satellite Sea Surface Temperature data over Southern European Seas in the framework of MyOcean project. *Rem Sens Env.* 2013 Oct; 129:1-16.
22. Kara BA, Helber RW, Boyer TP, Elsner JB. Mixed layer depth in the Aegean, Marmara, Black and Azov Seas: Part I: General features. *J Marine Syst.* 2009 Nov; 78:169-80.
23. Chen D, Busalacchi AJ, Rothstein LM. The roles of vertical mixing, solarradiation, and wind stress in a model simulation of the sea-surface temperature seasonal cycle in the tropical Pacific Ocean. *J Geophys Res.* 1994 Oct; 99(20):345-59.
24. Small RJ, deSzoek SP, Xie SP, O'Neill L, Seo H, Song Q et al. Air-sea interaction over ocean fronts and eddies. *Dyn Atmos Oceans.* 2008 Jul; 45(3-4):274-319.